Chapter 4. Photoemission Studies on Metal-Free Porphyrazine Compounds

4.1 Valence Region

The synthesis of metal-free tetraazaporphyrin, phthalocyanine and naphthalocyanine becomes easier upon substitution (addition) of tert-butyl (C_4H_9) groups. Therefore, a first step was to study the photoemission spectra of tert-butyl containing complexes in order to identify the effect of this substituent on the electronic structure of compounds. To that purpose, and also to facilitate the assignment of features in the photoemission spectra, both unsubstituted H_2Pc and P1-H_2 complexes were measured. Note that P1-H_2 compound is equivalent to H_2Pc with four peripheral hydrogen atoms substituted each by a tert-butyl group. For H_2Pc several theoretical works [OrB92, OCP96] and photoemission studies [Ber79, GFG94, OHI99] have been reported.

Peaks Assignment and Effect of Tert-butyl Substitution on the Photoemission spectra

Photoemission results on unsubstituted H_2Pc and P1-H_2 are presented in Fig. 4.1-1. The data were obtained with 90.6 eV photon energy. All spectra correspond to normal emission and an angle of incidence of 83° with respect to the surface normal. The light polarization was 80° with respect to the surface normal. For clarity the spectra are vertically displaced with respect to each other. The top spectrum corresponds to the H_2Pc and the bottom one to the P1-H_2 complex. The normalization of the spectra in the 30-40 eV binding energy range which is rather structureless appears reasonable for comparing relative intensity changes of the spectral features for the two compounds. The energy scale denotes electron binding energies with reference to the vacuum level.

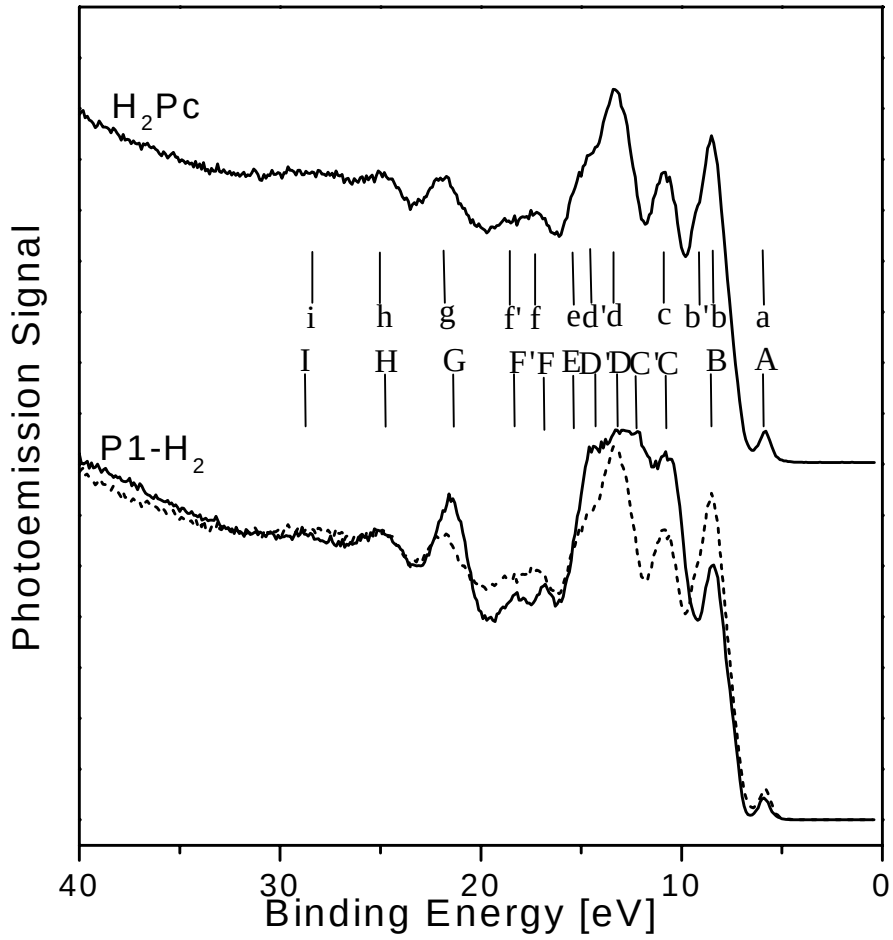

Fig. 4.1-1 Photoemission spectra from the unsubstituted H_2Pc film (top) and the P1-H_2 film (bottom), both obtained with 90.6 eV photon energy. Electron binding energies are given with respect to vacuum level, and intensities are normalized in the 30-40 eV binding energy range. The labels for the top spectrum directly correspond to the nomenclature in [OrB92]; the respective photoemission feature assignment is presented in Table 4.1-1. In order to account for binding energy changes, the bottom spectrum is labeled by the corresponding capital letters. The dashed spectrum at the bottom is identical to the top spectrum.

The binding energies were determined with respect to the vacuum level for thin films that also showed the substrate Au 4f core levels. From spectra measured with a negative bias applied to the sample (-10 V typical) was determined the low energy cut-off. Based on this, the binding energies were determined via $BE=h\nu-(E_{kin}-E_{cut\text{-}off})$, where $h\nu$, E_{kin}, and $E_{cut\text{-}off}$ represent the excitation energy, the kinetic energy and the low energy cut-

off of the spectrum. For thicker films, in order to compensate for charging, the binding energy scales were aligned to those obtained for the corresponding thin films.

There is good agreement between the H_2Pc spectrum and spectra reported in the literature for this compound (see e.g. [IKC80, SMK97]). However, better resolution is achieved in the experiments presented here.

In order to interpret the photoemission spectra, the binding energies of the photoemission features obtained in these experiments along with values reported in [OrB92] are listed in Table 4.1-1. The peak assignment is given in the top row. Small letters directly refer to Ref. [OrB92] while capital letters account for small shifts observed for P1-H_2. The notation used for the carbon and nitrogen atoms in the assignment indicates the different character of the respective atoms in the molecule, as shown in Fig. 4.1-2. Identical notations have been used in Ref. [OrB92].

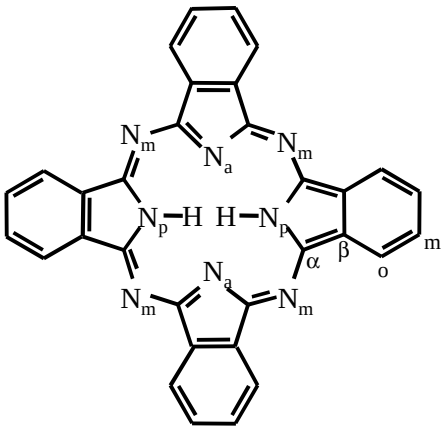

Fig. 4.1-2 Molecular structure of H_2Pc with the same notations as used in [OrB92] and for the peaks assignment. N_p indicates a pyrrole nitrogen, and N_a and N_m denote pyrrole aza and meso-bridging aza nitrogens, respectively.

The H_2Pc electronic structure can be viewed as the result of the addition of four benzene units to the central C_8N_8 ring [OrB88]. According to Table 4.1-1, the benzene contributions are found at the positions of bands **b**, **c**, **d**, **f**, **g**, and **h** while peak **a** at 5.9 eV binding energy originates exclusively from the HOMO of H_2Pc molecules.

Feature/ Species	**a (A)**	**b (B)**	**b‘**	**c (C)**	**C‘**	**d (D)**	**d‘ (D‘)**	**e (E)**	**f (F)**	**f‘ (F‘)**	**g (G)**	**h (H)**	**i (I)**
Assignment H_2Pc [OrB92]	$C_{2p}4a_{1u}$ (π), of Pc macrocycles	$C_{2p}1e_{1g}$ (π), N_m electron lone pairs*		$C_{2p}1a_{2u}$ (π), $C_{2p}2e_{2g}$ (σ), N_a electron lone pairs		C_{2s}-H_{1s} $1b_{1u}$ C_{2p}-H_{1s} $1b_{2u}$ C_{2p}-H_{1s} $2e_{1u}$		C_{2p}, N_{2p} central ring	C_{2s} $1e_{2g}$, C_{2p}-H_{1s} $2a_{1g}$	C_α2s	C_{2s} $1e_{1u}$	C_{2s} $1a_{1g}$	N_p2s, N_a2s
H_2Pc [GTG91] [TIK81]	5.9 5.9	8.5 8.6	- -	11.1 11.0	- -	13.5 13.6	- -	15.2 15.4	18.0 18.0	- -	21.8 21.9	24.9 24.9	28.2
H_2Pc [this work]	5.9	8.6	9.2	10.9		13.4	14.6	15.2	17.4	18.8	22.0	25.0	28.6
P1-H_2 [this work]	5.9	8.6		10.9	12.3	13.4	14.6	15.2	16.9	18.4	21.5	25.0	28.9

N_p=pyrrole nitrogen, N_a, N_m=pyrrole aza and meso-bridging aza nitrogens, respectively. C_α= carbon atom bound to N_p and N_m
*also N_p and N_a atoms, as results from Ref. [OCP96].

Table 4.1-1 Measured electron binding energies relative to vacuum level (in eV) for H_2Pc and P1-H_2 respectively, as obtained from **Fig. 4.1-1** and similar data. The corresponding error bars are 0.07 eV. For comparison and peak assignment, data reported in [OrB92] are also included. Labels in small letters refer to unsubstituted H_2Pc and capital letters refer to the P1-H_2 compound, respectively.

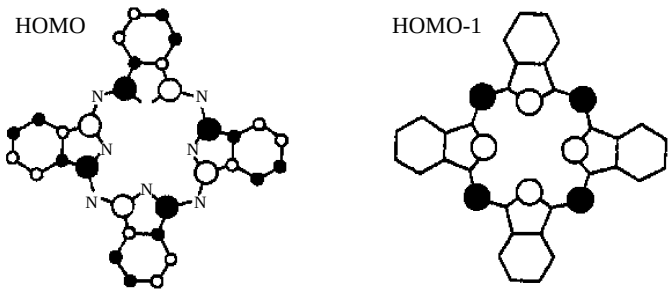

Fig. 4.1-3 The atomic orbital composition (marked by open and closed circles) of the two highest occupied molecular orbitals of H_2Pc, as taken from ref [OCP96].

The HOMO for H_2Pc spreads over the carbon backbone with negligible contributions from the meso-nitrogens, while the HOMO-1 is mostly localized on nitrogen atoms [OCP96]. A sketch of the atomic orbital composition of the HOMO and the HOMO-1 for H_2Pc is given in Fig. 4.1-3 [OCP96]. The largest contributions to HOMO come from the carbon atoms defining the inner carbon-nitrogen ring.

To facilitate the comparison between the photoemission features of P1-H_2 and H_2Pc, the spectra are plotted on top of each other in the bottom part of Fig. 4.1-1 (the dashed spectrum is just a copy of H_2Pc top spectrum). In this way, the effects in the photoemission spectrum due to the tert-butyl addition to the molecule appear explicitly. Largely, the values for the binding energy of the peaks are nearly the same for H_2Pc and P1-H_2. A small energy shift of about 0.4 eV towards lower binding energy is observed for the feature G. The influence of the four tert-butyl groups is predominantly manifested by an increase in the intensity of feature G and of the features found in the 9.5-16 eV binding energy range, relative to the band I. Feature A, which is derived from the HOMO, is found not to shift upon tert-butyl substitution. At this point it is worthwhile to mention also that only a slight shift (~6 nm) in the absorption maximum of the Q band is occurring upon tert-butyl substitution.

In contrast, for subphthalocyanine and its tert-butyl derivative theoretical calculations predicted that the tert-butyl slightly destabilizes the HOMO, yet the C atoms from tert-butyl do not contribute to the HOMO [FGG2001]. The subphthalocyanine is the lowest phthalocyanine homologues formed by three coupled isoindole moieties, with boron as the central atom.

He I spectra reported for the tert-butyl radical [KBS75, HoB79] show the presence of a wide band centered at about 6.92 eV binding energy, followed by narrower structures between 9-11 eV. The peak of maximum intensity is found at a binding energy of about 10.9 eV. However, in the present synchrotron-radiation photoemission spectra, the comparison between H_2Pc and P1-H_2 indicates stronger extra contributions due to tert-butyl substitution in the binding energy range from 10.2 and 12.4 eV.

The reason for the intensity decrease of features F, F' and B in P1-H_2 compared to H_2Pc is due to an increased background for the substituted compound as compared to the unsubstituted one. Therefore, the intensity of certain peaks (without tert-butyl contributions) relative to the background is smaller for P1-H_2 than for H_2Pc. As the normalization was done relative to the signal at ~32 eV binding energy, this explains the reduced intensity of the peaks B, F, and F' for P1-H_2 as compared to H_2Pc, in Fig. 4.1-1.

Evolution of the Photoemission Features as a Function of Ligand Size

Another important point in studying the set of metal-free compounds is to identify the changes in the structure of the valence region determined by the variation of the molecular structure. This refers to both the relative increase of the benzene features with enlargement of the ligand and to changes in the binding energy of the peak originating from HOMO.

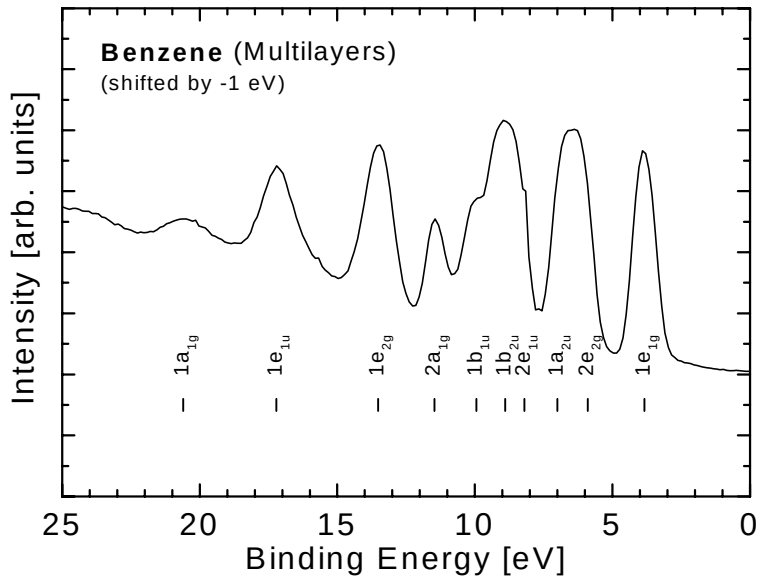

Fig. 4.1-4 Photoemission spectra of condensed benzene multilayers. The data are taken from Ref. [GTM98]. The spectra were obtained with 50 eV photon energy at normal light incidence.

For reference, Fig. 4.1-4 shows the photoemission spectra for condensed benzene multilayers, as taken from [GTM98].

The photoemission spectra of P0-H_2, P1-H_2 and P2-H_2 compounds are displayed in Fig. 4.1-5. Note that all complexes contain the same substituent, tert-butyl. They only differ by the number of benzo-units fused to the pyrrole group (zero, one or two). Excitation energy was 93.7 eV. The experimental geometry was the same as described for the H_2Pc and P1-H_2 measurements (see above).

The spectra were normalized with respect to the signal at ~32 eV binding energy. They have been vertically displaced with respect to each other and in order to facilitate the discussion, the P0-H_2 and P2-H_2 spectra have been displayed with the P1-H_2 spectrum overlapped on top of them.

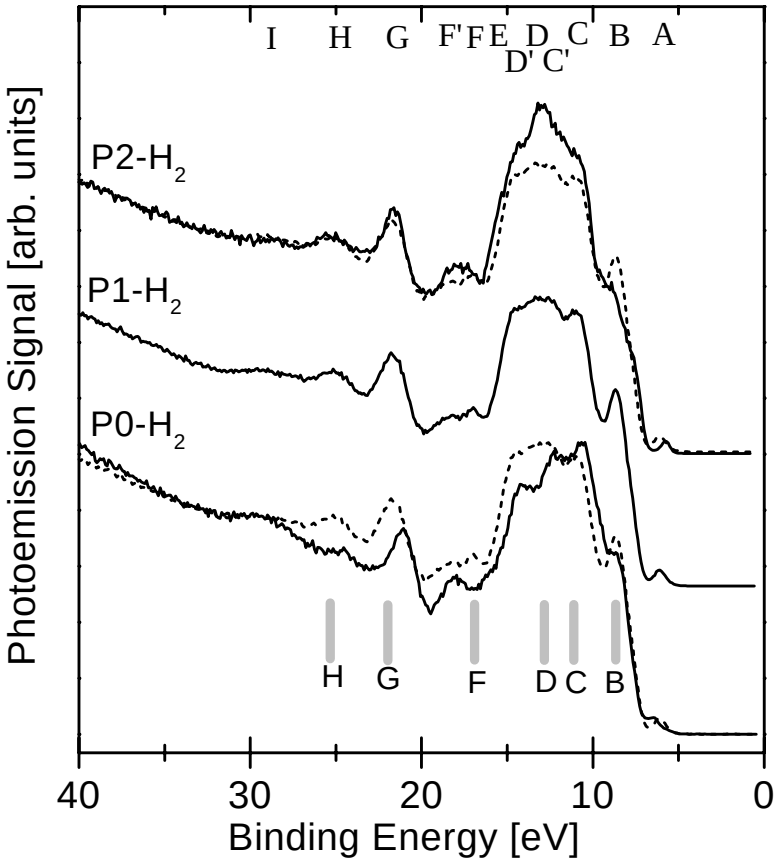

Fig. 4.1-5 Photoemission spectra of P0-H_2, P1-H_2, and P2-H_2 compounds. Electron binding energies are given with respect to the vacuum level. The dashed spectrum overlapped on the P0-H_2 spectrum and on the P2-H_2 spectrum is the spectrum of P1-H_2 compound (the middle spectrum in the figure), this being given for facilitating the comparison.

Starting out with P0-H_2, it should be noted that to our knowledge this is the first photoemission spectrum of the valence region reported in the literature for this compound. The film shows evidence for some photodegradation upon synchrotron-radiation exposure during the time necessary for obtaining a reasonable spectrum. It seems that the low-binding-energy region is mainly affected, particularly the bands A and B. Thus, in analyzing the spectrum it should be accounted for a possible broadening and smearing out of certain features (this type of changes are observed in the photoemission spectra after longer exposure times).

The assignment of the features of the P0-H_2 spectrum is based on the results from Table 4.1-1. The assignment can be done in a rather straightforward way by disregarding the respective benzene contributions and accounting for the tert-butyl ones (as P0-H_2 does not contain any benzene rings but has four tert-butyl groups). Since the phthalocyanine can be viewed as the result of four benzene rings added to the central carbon-nitrogen ring [OrB88, OrB92], the features of increased relative intensities for the next larger compound (P1-H_2) are directly assigned to benzene contributions (as also indicated in Table 4.1-1). The benzene spectral positions, deduced from this comparison and from Table 4.1-1, and also used to interpret the spectra of P1-H_2 and P2-H_2 molecules, are indicated by labels (shaded bars) in Fig. 4.1-5 (corresponding to peaks B, C, D, F, G and H, respectively). Most of the photoemission features of P0-H_2 are shifted to lower binding energies with respect to those of P1-H_2 by an amount between 0.4 and 0.8 eV. This is most probable due to the fact that they include contributions from the central porphyrazine ring and pyrrole moieties but no contributions from the benzene units. Peak F' stays at fixed energy as it originates from the carbon atoms found in the central ring of the molecule, C_α2s (see Fig. 4.1-2 and Table 4.1-1). Feature A is found at larger binding energy relative to the P1-H_2 case. The higher intensity of feature C in the P0-H_2 spectrum compared to the P1-H_2 spectrum is due to the normalization at 32 eV (the signal at this binding energy being larger for P1-H_2 than for P0-H_2).

Several theoretical studies [GGA94, LaP96, THN96, GhV97] have been performed with the aim of determining the electronic structure of metal-free tetraazaporphyrin (H_2TAP) but to our information not for the tert-butyl substituted one. However, to our knowledge, experimental valence-band spectra were missing for both metal-free tetraazaporphyrin or tert-butyl substituted metal-free tetraazaporphyrin. Calculated energies for the molecular orbitals of isolated H_2-tetraazaporphyrin molecule are summarized in Table 4.1-2.

	[GGA94] double-ζ basis set	[GGA94] polarized double-ζ basis set	[LaP96]	[THN96]	[GhV97]
HOMO	a_u 6.53	a_u 6.25	a_u 4.94	a_u 6.98	a_u 7.83
HOMO-1	b_{1u} 8.73	b_{1u} 9.03	b_{1u} 5.40	b_{1u} 9.147	b_{1u} 8.38
HOMO-2	b_{2g} 9.82	b_{2g} 9.83	b_{1g} 5.48	b_{3g} 10.113	b_{2g} 8.60
HOMO-3	b_{1u} 10.04	b_{1u} 10.04	b_{2g} 5.52	b_{1u} 10.297	b_{3g} 9.28

Table 4.1-2 Binding energies in eV and orbital symmetries as determined from calculations of the electronic structure for unsubstituted metal-free tetraazaporphyrin.

Similar to the H_2Pc case, it is found that the HOMO is given by the carbon atoms within the macrocycle while the HOMO-1 is mostly due to nitrogen contributions [OCP96].

In the present experiments, the binding energy of peak A, which originates from the HOMO of P0-H_2, is located at 6.57±0.07 eV, which is closer to the predicted values in Ref. [GGA94] and [THN96].

Following the same analysis as done for the P0-H_2 and P1-H_2 spectra, one can trace the changes of the photoemission features in going from the P1-H_2 to the P2-H_2 compound. Except for feature B, the intensity of peaks containing benzene contributions increases and, except for peak A, no peak shifts are observed. Peaks F and F' are not resolved anymore. These features evolve into a broad peak. The reason for the intensity decrease of feature B in P2-H_2 relative to P1-H_2 compound is likely the same as mentioned when comparing band C for P1-H_2 and P0-H_2 (an increase in the background for P2-H_2, this influencing the signal at the position where the normalization is done). Similar to the H_2Pc case, from the point of view of the electronic structure, naphthalocyanine (equivalent to P2-H_2 without tert-butyl substitution) can be viewed as formed by joining four naphthalene moieties to the central carbon-nitrogen ring [OCP93, OPC93]. The assignment of the peaks can be done based on Ref. [OrB92, OCP93, OCP96]. Band A is given by the HOMO, this orbital having similar composition with that for H_2Pc (Fig. 4.1-3). Band B contains contributions from π molecular orbitals in naphthalene and also from N atoms, while band C includes σ and π molecular orbital contributions as well as emission from nitrogen atoms. The contributions of naphthalene moieties to the remaining spectral features are largely of σ character. In order to have a correct assignment it should also be accounted for the tert-butyl signal in the composition of spectral features. Theoretical calculations [OCP96]

predict a HOMO to HOMO-1 separation in metal-free naphthalocyanine (H_2Nc) of 2.51 eV. It was also calculated that the energy of the HOMO decreases by 0.37 eV in passing from H_2Pc to H_2Nc. The symmetry for HOMO and HOMO-1 is identical for H_2Nc, namely a_u.

According to Ref. [OCP96], the b_{1u} HOMO-1 of H_2Pc is not influenced by the extension of the macrocycle (is localized only on nitrogen atoms) and therefore the molecular orbitals with this composition are found at identical energy in H_2Pc, H_2Nc, and H_2Ac. We thus conclude that in the present photoemission spectra these particular molecular orbitals give photoemission signal (in addition to benzene contributions) at the position of band B.

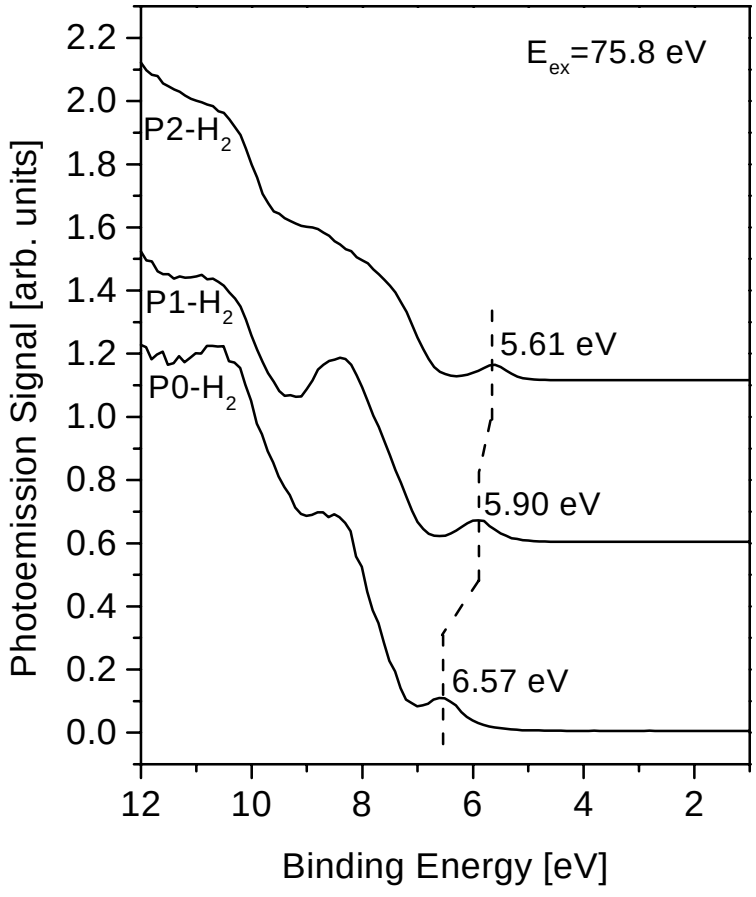

Fig. 4.1-6 Photoemission spectra of P0-H_2, P1-H_2 and P2-H_2 compounds at the edge of the valence region. The binding energy of feature A (HOMO) decreases with the extension of the π-electron system of the molecule. Labels mark the respective HOMO binding energies.

To compare the experimental binding energies of band A (HOMO) for the different molecules, a zoom of the edge of the valence region is shown in Fig. 4.1-6. All spectra have been measured with a photon energy of 75.8 eV. There is a noticeable decrease in the binding energy of the feature derived from the HOMO with increasing ligand size. The HOMO binding energies for this series of compounds are determined to be 6.57±0.07 eV for P0-H_2, 5.9±0.07 eV for P1-H_2 and 5.61±0.07 eV for the P2-H_2 compound. The error bars are equal with the standard deviations that resulted from the measurements of several thin films for each material.

These values are in good agreement with theoretical studies, which predicted that the linear benzoannelation causes a decrease of the first ionization potential of the molecule. The fact that the P0-H_2 spectrum is available in the current study allows now a detailed comparison. It is noted, however, that the theoretical HOMO energy values calculated for isolated unsubstituted molecules of H_2-tetraazaporphyrin (H_2TAP), H_2-phthalocyanine (H_2Pc), and H_2-naphthalocyanine (H_2Nc) [OPC90, GGA94, OCP96] are usually lower than the experimental ones determined for thin films. In order to facilitate comparisons between the experimental and theoretical results, an rigid up shift of the theoretical energy scale has to be considered for most of the cases.

The destabilization of HOMO with linear benzoannelation is attributed to the antibonding interactions with the fused units. The HOMO remains mainly localized on the central tetraazaporphyrin (porphyrazine) ring. The antibonding interactions become larger at the addition of each benzo-unit but the contributions of the outermost benzene rings to the HOMO decrease as the number of benzene rings increases [OCP96]. Thus, the antibonding interactions do not increase linearly with the number of benzo-units, the effect being the stronger the closer the benzo-unit is to the central porphyrazine ring.

The HOMO binding energies extracted from the present measurements are summarized in Table 4.1-3. E_{abs}- the energies corresponding to the absorption maxima for the lower energy component of the Q band when the compounds are dissolved in benzene (Q band appears split for P0-H_2 and P1-H_2 in solution) are also indicated. The wavelengths of the absorption maxima are measured with accuracy better than 1 nm. For comparison, the computed energy values for HOMO and LUMO of the molecules without tert-butyl are added from Ref. [OCP96]. It is considered that the P0-H_2 film had no significant photodegradation, so that the initial peak positions were not affected. A tentative value for the LUMO binding energy is determined as $E_{LUMO}=E_{HOMO}-E_{abs}$.

Compound	HOMO[1),2)] [eV]	Energy corresponding to 1st absorption maximum in benzene [eV] (E_{abs})	LUMO[1),3)] [eV]	HOMO[1),4)] [eV]	LUMO[1),4)] [eV]
P0-H_2	6.57±0.07	2	4.57	7.3	5.22
P1-H_2	5.9±0.07	1.78	4.12	6.42	4.61
P2-H_2	5.61±0.07	1.59	4.02	6.05	4.4

[1)] energies relative to the vacuum level; [2)] determined for the solid films; [3)] assuming for simplicity that $E_{LUMO}=E_{HOMO}-E_{abs}$ [4)] From Ref. [OCP96], calculated for the corresponding compounds without tert-butyl substitution

Table 4.1-3 Measured binding energies for feature A (HOMO) together with the values corresponding to the 1st absorption maximum of the compound dissolved in benzene. Assuming for simplicity that $E_{HOMO}-E_{abs}=E_{LUMO}$, an approximate value for the LUMO binding energy can be determined. For comparison, the computed energy values for HOMO and LUMO, determined for the compounds without tert-butyl substitution in [OCP96], are also given.

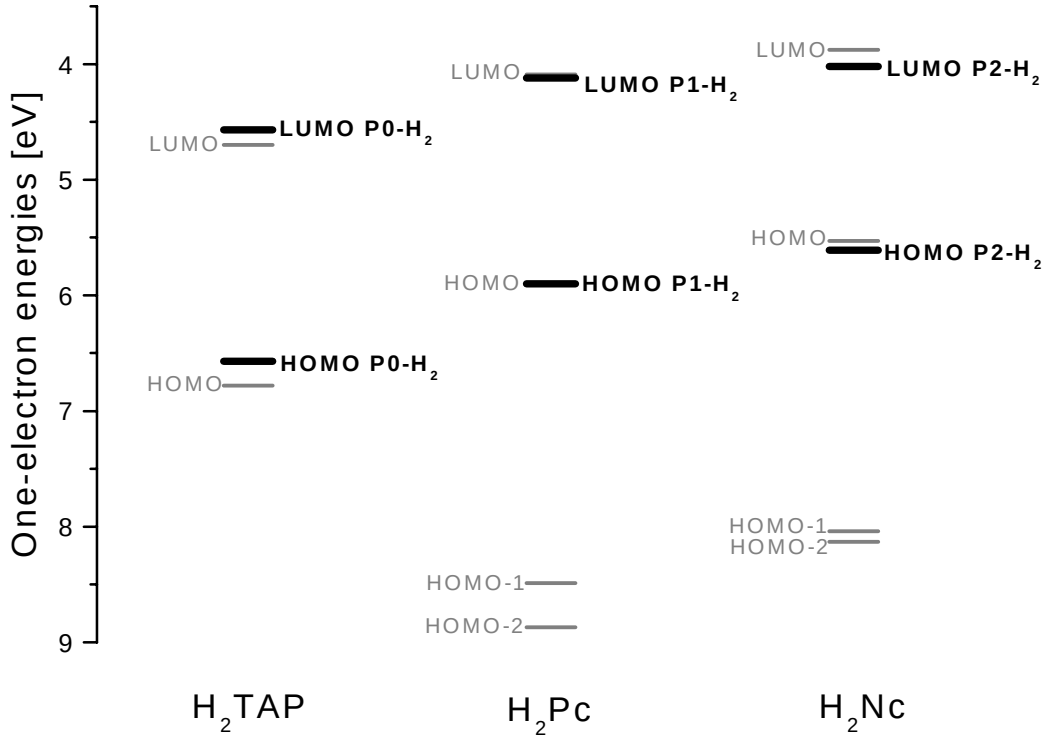

Fig. 4.1-7 Comparison between the one-electron energy levels obtained in ref. [OCP96] for metal-free tetraazaporphyrin (H_2TAP), metal-free phthalocyanine (H_2Pc), metal-free naphthalocyanine (H_2Nc) and HOMO and LUMO binding energies deduced in the present experiments for P0-H_2, P1-H_2, and P2-H_2. The theoretical energy scale was shifted by 0.52 eV in order to align the theoretical energy of HOMO for H_2Pc with the experimental binding energy for P1-H_2. Thick lines symbolize the experimental data while thinner lines symbolize the theoretical values.

Fig. 4.1-7 graphically summarizes the theoretical energy levels from Ref [OCP96] for metal-free tetraazaporphyrin (H_2TAP), metal-free phthalocyanine (H_2Pc), and metal-free naphthalocyanine (H_2Nc), and the experimental HOMO and LUMO positions obtained in the present measurements for P0-H_2, P1-H_2, P2-H_2.

The calculations in [OCP96] were performed for isolated molecules and therefore, in Fig. 4.1-7 the theoretical energy scale is shifted by 0.52 eV, in order to align the theoretical value of H_2Pc HOMO energy with the experimental value for P1-H_2. Hence, the theoretical values in Table 4.1-3 differ by that amount (0.52 eV) in Fig. 4.1-7. The agreement between the theoretical HOMO and LUMO energies for the non-substituted compounds and the experimental HOMO and LUMO energies for the tert-butyl containing complexes is reasonable good. This suggests once more that the effect of tert-butyl on the electronic structure of the porphyrazine macrocycle is only minor.

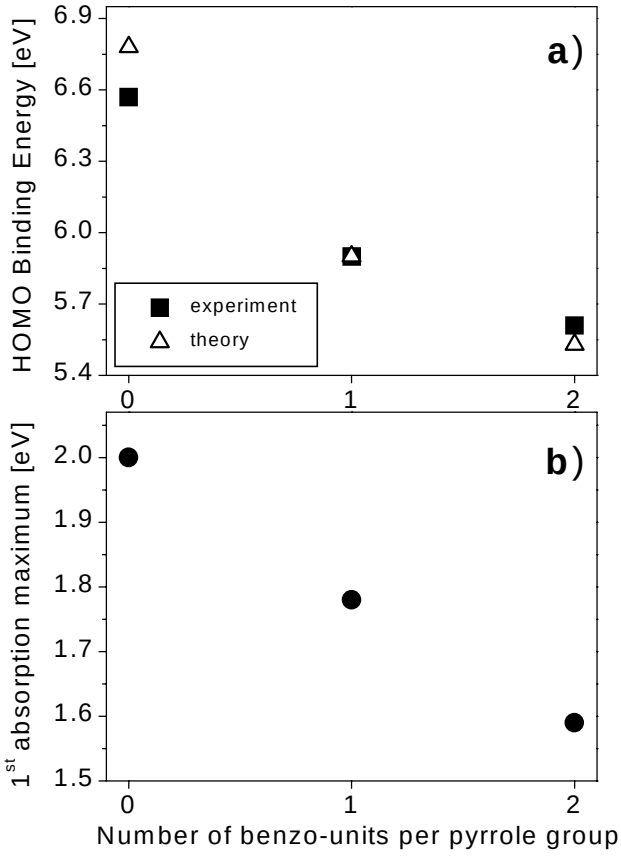

Fig. 4.1-8 (a) Experimentally determined HOMO binding energies (solid squares) as a function of the number of benzo-units fused per pyrrole group for P0-H_2, P1-H_2 and P2-H_2. The corresponding theoretical values obtained in Ref. [OCP96] for nonsubstituted compounds and shifted by 0.52 eV are added for comparison (open triangles). (b) Dependence of the 1st absorption maximum measured in benzene as a function of the number of benzo-units fused per pyrrole group for P0-H_2, P1-H_2 and P2-H_2.

Fig. 4.1-8(a) shows the binding energy change of feature A (HOMO) as function of the number of benzene units fused per pyrrole group for P0-H_2, P1-H_2, and P2-H_2. The dependence is similar to that predicted by Orti and coworkers for nonsubstituted compounds [OCP96], the theoretical values shifted by 0.52 eV being marked by open triangles in Fig. 4.1-8(a). Fig. 4.1-8(b) displays the dependence of the characteristic absorption maximum measured in benzene as a function of the number of benzene units fused per pyrrole group for P0-H_2, P1-H_2 and P2-H_2.

4.2 Photodegradation Effects

An aspect that should be always taken into account when analyzing photoemission data from organic compounds is the possible photodegradation of the sample caused by the interaction with light or secondary electrons. For that reason several investigations have been performed to quantify the effects of sample exposure to synchrotron radiation.

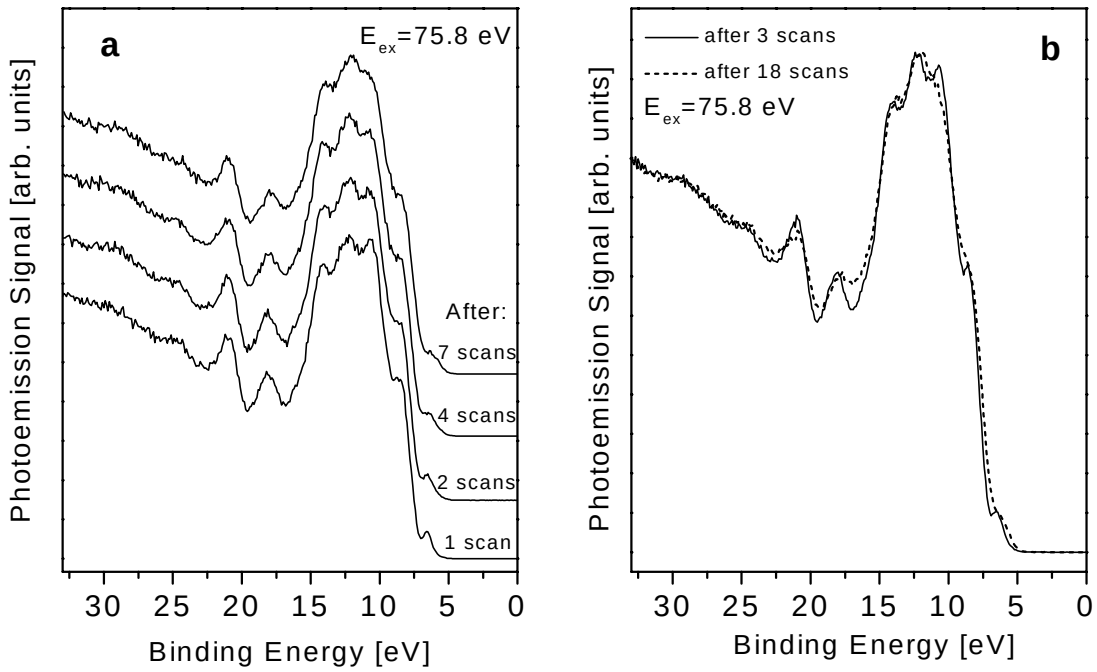

Fig. 4.2-1 Changes in the photoemission spectra of the P0-H_2 compound due to synchrotron radiation exposure. (a) spectra measured on the same spot and vertically translated for clarity. (b) two overlapped spectra measured after different beam exposure times, again on an identical spot, but one that is different from that in figure (a).

P0-H_2 is the most sensitive metal-free compound in the series to synchrotron radiation exposure, its photoemission spectrum showing noticeable spectral changes. This is depicted in Fig. 4.2-1(a), where several photoemission spectra have been taken one after the other from an identical spot. Changes in the photoemission features occur to a certain degree even within the time necessary to obtain a single scan (approximately 2 minutes). Fig. 4.2-1(b) presents an overlap of spectra taken from an identical spot (but one that is different from that in figure 'a'), at different exposure times.

The photodegradation of the sample manifests itself by the broadening and smearing out predominantly of features A, B, C but also G and F. Investigations as to the nature of the photodegradation were not performed in these studies. Anyway, it is noteworthy that after longer synchrotron radiation exposure of the sample (around one hour), the exposed spot of a P0-H_2 thick film (initially dark violet) becomes light in color.

The effects of the synchrotron light on the P1-H_2 compound are weaker and spectral changes were observed only after longer exposure times than for the P0-H_2 compound. These changes are largely characterized by a broadening of peaks A, B, F, F' and G (Fig. 4.2-2).

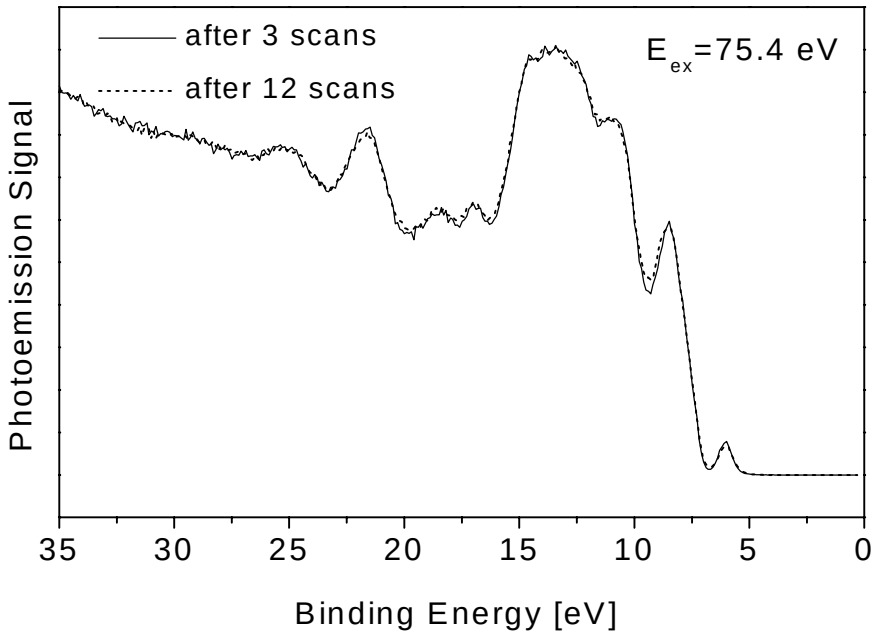

Fig. 4.2-2 Photoemission spectra of the P1-H_2 compound for two different synchrotron radiation exposure times. The photon energy was 75.4 eV.

The P2-H_2 compound appears to be even less affected by the synchrotron radiation exposure than P1-H_2. For this reason the spectra taken at different exposure times are not shown here for P2-H_2.

From the above considerations it is concluded that synchrotron light exposure seems mainly to affect the atoms located in the central porphyrazine ring, the photodegradation effects induced by the synchrotron beam decrease when going from the smaller to the larger molecules in the series.

4.3 Summary

This chapter presents the results of photoemission measurements on the set of metal-free porphyrazine molecules. In this way the ligand features in the spectra were identified and serve as reference for comparison with spectra of metal-containing complexes. The evolution of the valance band features with increase of ligand size was investigated and the assignment of the peaks was done based on the existing literature. The decrease of the HOMO binding energy with stepwise linear benzoannelation was also evaluated in this system of porphyrazines.